Spatial effects of HF multiple scattering in the ionosphere: Experimental observations

Nikolay Zabotin[1,2] and Terence Bullett[1,3]

Received 3 January 2011; revised 15 May 2011; accepted 25 May 2011; published 27 August 2011.

[1] The theory of multiple scattering of MF/HF radio waves by intermediate-scale (0.1–5 km) ionospheric irregularities predicts a very distinctive distribution of the relative integral intensity of a signal reflected from the ionosphere in the vicinity of a ground-based transmitter. It is significantly reduced within a distance of about several tens of kilometers. A ring of enhancement occurs at a greater distance. At still larger distances from the transmitter, effects of multiple scattering are weakened and the integral intensity returns to its undisturbed value. While there are experimental confirmations of the "anomalous attenuation" effect near the transmitter location, no attempt has yet been made to track the intensity features at the larger distances. This paper presents results of the first experimental campaign of this kind that was conducted in September–November 2009 in and around Boulder, CO. The results obtained confirm that significant deviations from the predictions of geometrical optics occur, and these deviations are in general agreement with the theory of multiple scattering in the ionosphere.

Citation: Zabotin, N., and T. Bullett (2011), Spatial effects of HF multiple scattering in the ionosphere: Experimental observations, *Radio Sci.*, *46*, RS4009, doi:10.1029/2011RS004645.

1. Introduction

[2] Intermediate-scale (0.1–5 km) electron density irregularities stretched along the magnetic field lines are a prominent structural property of the ionosphere. Their statistical description is accomplished with two basic parameters, the amplitude $\Delta N/N$ and the index ν of their transversal power spectrum. In spite of their usually low amplitudes (ΔN/N on the order of 1 percent or less) these irregularities influence natural and artificial HF signals propagating in the ionosphere in several ways. In vertical sounding of the ionosphere, the optical thickness for scattering by the intermediate-scale irregularities is frequently considerably greater than unity [*Bronin et al.*, 1993, 1996]. This implies a multiplicity of the scattering that may cause spatial and angular redistribution of the radio radiation flux propagating through the ionosphere. The theory of this phenomenon has been developed. The rigorous study starts from the radiative transfer equation (RTE) for magnetized irregular plasma [*Bronin and Zabotin*, 1992] that mathematically describes signal propagation in the multiple-scattering regime. *Zabotin* [1993] and *Bronin and Zabotin* [1993] suggested a modification of the RTE for a plane plasma layer, having an analytic solution in the approximation of small-angle scattering in the invariant ray coordinates (SASIRC). Using this approach, it was shown that the mean intensity and the arrival angles of the HF signal reflected from the ionosphere can be significantly altered, resulting, in particular, in an anomalous attenuation (AA) effect near a ground-based transmitter and in anomalous refraction (AR) effect [*Zabotin et al.*, 1998a; *Bronin et al.*, 1998; *Zabotin et al.*, 1998b; *Kovalenko and Zabotin*, 1999; *Zabotin and Kovalenko*, 1999; *Bronin et al.*, 1999; *Zabotin et al.*, 2001, 2004].

[3] Note that the term "small-angle scattering" relates to the most probable direction of scattering, and the term "multiple scattering" (as opposed to the "single scattering") relates to the intensity of this process, so both terms may be required to characterize the same situation. Predominantly small-angle character of the ionospheric scattering results from the relationship between the wavelength (of the order of 10–100 m) and the irregularity's transversal scale length (of the order of 1 km), which is substantially larger than the wavelength, but still smaller than the first Fresnel zone scale length (the latter being of the order of few km, thus requiring the scattering theory language rather than the geometrical optics description). The small-angle character causes another interesting feature of the ionospheric scattering: the large optical thickness does not necessarily entail a loss of the phase coherence. This explains how some wave phenomena requiring phase coherence, like the artificial periodic inhomogeneities [*Belikovich et al.*, 1997], can coexist with the multiple scattering. Relative stability of the phase fronts in conditions of the small-angle scattering is a general property of wave propagation in various random media [see *Godin*, 2009].

[4] Anomalous attenuation in HF vertical sounding of the ionosphere in natural conditions has long been an experimental fact. It was described in terms of an increased *effective* electron collision frequency [*Setty et al.*, 1970, 1971; *Setty*, 1972; *Vodolazkin et al.*, 1993; *Denisenko et al.*, 1987], compared to the true gas-kinetic value in the ionospheric

[1]CIRES, University of Colorado at Boulder, Colorado, USA.
[2]CET, ECEE, University of Colorado at Boulder, Boulder, Colorado, USA.
[3]NGDC, NOAA, Boulder, Colorado, USA.

0048-6604/11/2011RS004645

F region. However, careful analysis showed absence of a collisional mechanism able to provide the observed attenuation. Multiple-scattering theory provides the necessary explanation. The anomalous attenuation effect has also been confirmed by dynasonde results [*Zabotin et al.*, 2004].

[5] Anomalous attenuation of pump and probe waves of *extraordinary* polarization in ionosphere heating experiments is a very compelling evidence of multiple scattering theory. Anomalous absorption of *ordinary* waves in ionospheric "heating" is well known, and has been explained at least in part by a mode conversion mechanism [*Vas'kov and Gurevich*, 1975; *Jones et al.*, 1984]. But mode conversion cannot occur for extraordinary waves. Their anomalous attenuation can be explained by multiple scattering from the kilometer-scale irregularities caused by heating. An early result [*Yerukhimov et al.*, 1980] was consistent with this view. Experimental results of *Boiko et al.* [1984, 1985] also may be explained using the multiple scattering mechanism. A successful dedicated experimental test has been done using the Sura heating facility [*Zabotin et al.*, 2002].

[6] Experimental data on the anomalous refraction effect (changes of arrival angle of a wave on a short baseline, when the transmitter to receiver distance is about 100 km) are reported by *Baulch et al.* [1984].

[7] Solution of the transfer equation [*Zabotin et al.*, 1998a] predicts a characteristic spatial distribution of the integral intensity of the received signal on the ground level. It is reduced in the vicinity of a ground-based radio source and some enhancement occurs as the distance from the transmitter increases. At still larger distances from the transmitter, effects of multiple scattering are weakened and the integral intensity returns to its undisturbed value. A qualitative explanation for this effect is the following. In the case of multiple scattering a redistribution of the full energy flux occurs. Unlike single scattering situation, all portions of energy participate in the scattering many times. As a result, the energy flux near vertical direction is "scooped out," and this energy returns to the ground farther away from the transmitter. This conforms to the energy conservation: there is a spatial redistribution by scattering in the ionospheric layer, but not a dissipative absorption. There is an azimuthal dependence of the effect as a consequence of geomagnetic field asymmetry together with the assumed field alignment of plasma irregularities.

[8] This kind of spatial redistribution of the radiation flux is an important and unique consequence of the theory, it is inherent to the nature of scattering processes (where no energy losses occur). Experimental confirmation of this prediction would be of utmost significance for validation of the theory. In this paper we report results of an experiment to confirm the spatial effect of the multiple scattering conducted in 2009–2010 in the vicinity of Boulder, Colorado and using Boulder VIPIR (Vertical Incidence Pulsed Ionosphere Radar) system together with a mobile setup of a digital radio sensor. Our theoretical approach is described briefly in section 2. Details of the experiments are stated in section 3. In section 4 the basic stages of the data processing are presented. Sections 5 and 6 summarize results and conclusions.

2. Theoretical Estimates

[9] In our theoretical calculations we have adopted an approach stated by *Zabotin et al.* [2004], who obtained solution of the radiative transfer equation in the approximation called SASIRC (Small-Angle Scattering in the Invariant Ray Coordinates). The solution is expressed in terms of the angular distribution of the sky radio brightness $P(\theta, \varphi, \vec{\rho})$ for an observer at some point $\vec{\rho}$ on the ground (θ, φ are zenith and azimuth angles defined at this point and called "invariant ray coordinates" in the theory and $\vec{\rho}$ is a two-dimensional vector in a magnetically oriented coordinate system which origin $\vec{\rho}=0$ corresponds to the transmitter location). In a simplified version of the theory, propagation and scattering of radio waves in ionospheric plasma are treated neglecting effects of geomagnetic field. However, it is taken into account that irregularities of the plasma density are stretched along the magnetic field lines. This is why the results still depend on the dip angle of the geomagnetic field and on geographic location. What follows in this section is a short summary of some theoretical results stated in the earlier publications in greater detail.

[10] Field-aligned ionospheric irregularities are characterized by a realistic three-dimensional spectrum,

$$F(\vec{\kappa}) = C_A\left(1+\kappa_\perp^2/\kappa_{0\perp}^2\right)^{-\nu/2}\delta(\kappa_\parallel), \tag{1}$$

where $\kappa_\perp$ and $\kappa_\parallel$ are the vector $\vec{\kappa}$ (irregularity spatial harmonic) components orthogonal and parallel to the magnetic field lines; $\kappa_{\perp 0} = 2\pi/l_{0\perp}$; $l_{0\perp}$ is the outer scale of the irregularity spectrum; ν is the spectrum index; $\delta(x)$ is the Dirac delta function; and C_A is a normalizing constant that may be found from the condition of equality of the root-mean-square irregularity amplitude $\Delta N/N$ at a transversal scale length R, to some value δ_R. A strict formulation of the condition determining C_A is based on application of the structure function [*Zabotin et al.*, 1998a; *Zabotin and Wright*, 2001].

[11] The influence of multiple scattering on the spatial distribution of signal energy on the ground is characterized by the quantity $L(\vec{\rho}) = P(\vec{\rho})/P_0(\vec{\rho})$, where $P(\vec{\rho})$ is the total intensity (the sky radio brightness integrated over all angles) in presence of scattering and $P_0(\vec{\rho})$ is the total intensity at the same point in absence of scattering (when $\Delta N/N = 0$).

[12] The theory gives the following expression for $L(\vec{\rho})$ (for details, see *Zabotin et al.* [2004]):

$$L(\vec{\rho}) = \frac{(2H+h_0)^2}{\pi^2}\frac{P_0(0)}{P_0(\vec{\rho})}\int\int dxdy\frac{\tan\left(\sqrt{x^2+y^2}\right)}{\sqrt{x^2+y^2}} \cdot \int\int d^2q\, F(\vec{q},\theta,\varphi), \tag{2}$$

where H is the distance from the layer base at h_0 to the height of reflection for a plasma density layer that is assumed to be linear ($z = H\cdot X + h_0$; $X = \omega_e^2/\omega^2$; ω_e is the plasma frequency; $\omega = 2\pi f$, and f is the radio frequency); $x = \theta\cos\varphi$ and $y = \theta\sin\varphi$; and

$$F(\vec{q},\theta,\varphi) = \cos[\vec{q}\cdot\vec{\rho}_0(\theta,\varphi) - \vec{q}\cdot\vec{\rho} - I_s(\vec{q},\theta,\varphi)]\exp[I_c(\vec{q},\theta,\varphi)],$$

$$I_s(\vec{q},\theta,\varphi) = \int dz\iint d\theta'\,d\varphi'\sin\left[\vec{q}\cdot\vec{\Phi}(z,\theta,\varphi,\theta',\varphi')\right]Q(z,\theta,\varphi,\theta',\varphi'),$$

$$I_c(\vec{q},\theta,\varphi) = \int dz\iint d\theta'\,d\varphi'\left\{\cos\left[\vec{q}\cdot\vec{\Phi}(z,\theta,\varphi,\theta',\varphi')\right]-1\right\} \cdot Q(z,\theta,\varphi,\theta',\varphi').$$

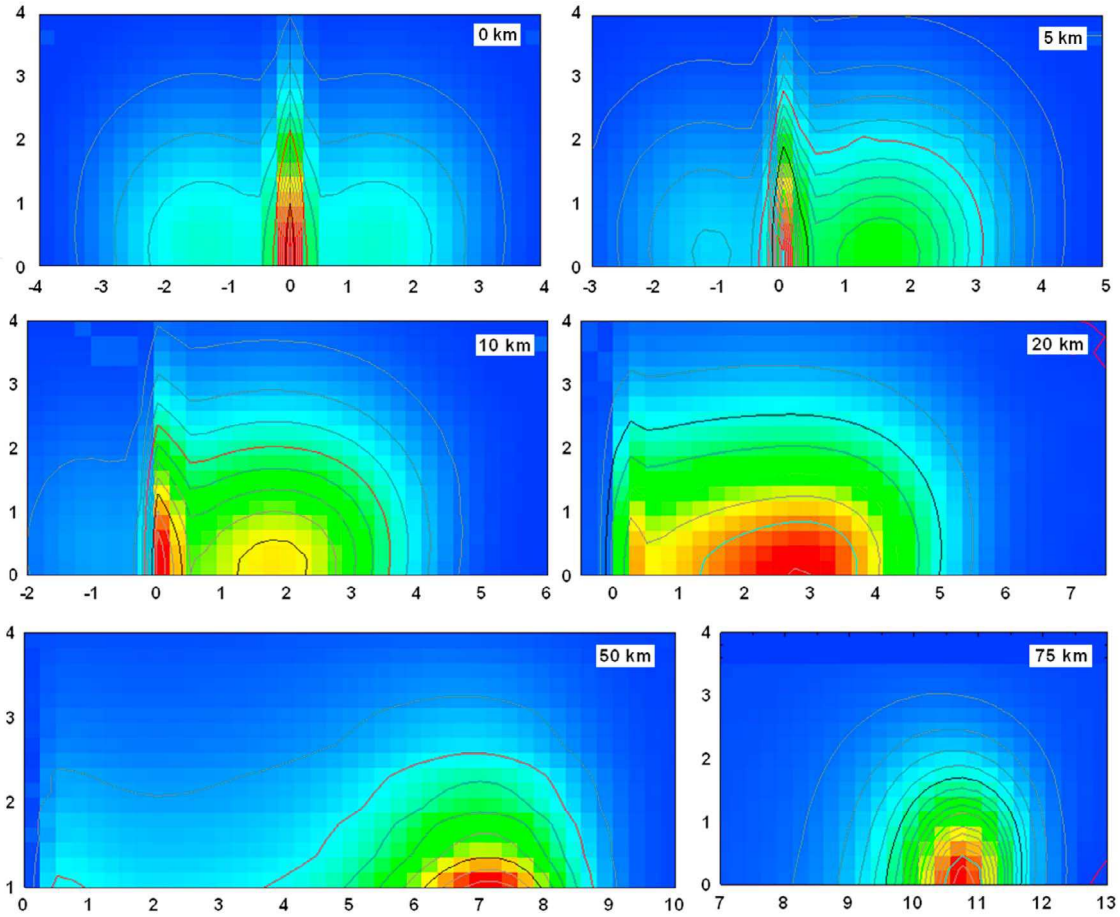

Figure 1. Angular distribution of the sky radio brightness $P(\theta, \varphi, \vec{\rho})$ in relative units (blue corresponds to the minimum value; red corresponds to the maximum value) for a receiver position shifted magnetic eastward from the transmitter, for several shift distances ($|\vec{\rho}| = 0$, 5, 10, 20, 50, 75 km), and for kilometer-scale irregularity amplitude $\Delta N/N = 0.005$, at the latitude of Boulder. Horizontal and vertical axes show zenith angles in the east-west and in the south-north directions, respectively.

[13] Integration over z is carried out along ascending and descending branches of the raypath corresponding to the invariant coordinates θ, φ. The vector function $\vec{\Phi}(z, \theta, \varphi, \theta', \varphi')$ represents the displacement of the arrival point at the ground of a ray which has invariant angular coordinates θ', φ', after scattering at the level z, relative to the arrival point of an incident ray with invariant angular coordinates θ, φ. The scalar function

$$Q(z, \theta, \varphi, \theta', \varphi') = \sigma(\theta, \varphi, \theta', \varphi') C^{-1}(z, \theta, \varphi) \sin\theta' |d\Omega_k'/d\Omega'|$$

contains the differential scattering cross section $\sigma(\theta, \varphi, \theta', \varphi')$; $C(z, \theta, \varphi)$ is the cosine of the inclination angle to the axis of a raypath corresponding to the invariant angles θ, φ;$|d\Omega_k'/d\Omega'|$ is the Jacobian of the coordinate transformation from the current zenith and azimuth angles of the wave vector to the invariant ray variables θ', φ'.

[14] In isotropic plasma the differential scattering cross section has the following simple form:

$$\sigma(\theta, \varphi, \theta', \varphi') = 0.5\pi k_0^4 X^2 \, F(\Delta\vec{\kappa}),$$

where $k_0 = 2\pi f/c$, $F(\vec{\kappa})$ is the spatial spectrum of irregularities (already mentioned above), and $\Delta\vec{\kappa}$ is the scattering vector that may be expressed through the invariant variables $\theta, \varphi, \theta', \varphi'$.

[15] Figure 1 shows angular distribution of the sky radio brightness (ray intensity $P(\theta, \varphi, \vec{\rho})$) for a receiver position shifted eastward from the transmitter's magnetic meridian plane, for several shift distances, and for kilometer-scale irregularity amplitude $\Delta N/N = 0.005$, at the latitude of Boulder. Qualitative properties of such distributions were first described by *Zabotin et al.* [2004]. With increasing shift, the nearer-side maximum gradually becomes dominant, but the former central peak continues to play a noticeable role up to some distance. Characteristic three-to-two-maxima structure of the obliquely reflected signal suggests some similarity to the double refraction. This effect is not of magnetoionic nature per se; it is caused by the multiple scattering from field-aligned irregularities. Note that in absence of scattering (when $\Delta N/N = 0$) the angular distribution of the sky radio brightness would be merely a delta function with a peak θ, φ at corresponding to a single raypath connecting the transmitter and the receiver.

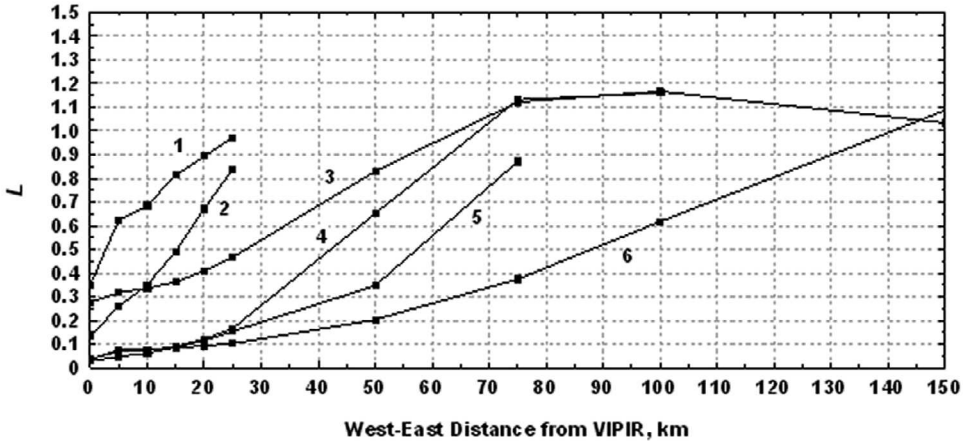

Figure 2. Plots show relative effectiveness of spatial redistribution of radio energy flux $L(\vec{\rho})$ caused by multiple scattering as a function of the distance to source in the west-east direction for several sets of parameters: 1, $f = 2570$ kHz, $\nu = 2.2$, $\Delta N/N = 0.005$, $H = 50$ km; 2, $f = 2050$ kHz, $\nu = 2.7$, $\Delta N/N = 0.01$, $H = 20$ km; 3, $f = 2570$ kHz, $\nu = 2.7$, $\Delta N/N = 0.005$, $H = 50$ km; 4, $f = 2050$ kHz, $\nu = 2.7$, $\Delta N/N = 0.02$, $H = 20$ km; 5, $f = 2727$ kHz, $\nu = 2.7$, $\Delta N/N = 0.005$, $H = 50$ km; 6, $f = 2570$ kHz, $\nu = 3.5$, $\Delta N/N = 0.005$, $H = 50$ km.

[16] Total power of the signal reflected from the ionosphere and the parameter $L(\vec{\rho})$ describing effectiveness of the multiple scattering may be obtained by integration of the distribution $P(\theta, \varphi, \vec{\rho})$ over the angles. Examples of the results of this kind are shown in Figure 2 as a function of the distance to the magnetic meridian plane where the source is located.

[17] As it follows from the typical theoretical calculations illustrated in Figure 2, the effect of multiple scattering is characterized by a gradual increase in the relative signal intensity with the distance to the source growing within few to one hundred kilometers range, compared to its undisturbed values predicted by the ray theory. As we shall see later, the ray tracing calculations, even taking into account the collisional losses in the D region, usually predict either no significant change or a slight decrease of the absolute signal intensity within the ~100 km distance. So observing nearly constant or growing values of the absolute intensity (of the amplitude) of the signal at increasing distances may serve as an indicator of multiple scattering in the ionosphere.

3. Experiment Setup

[18] The first question that had to be resolved for this project is what source of HF signal to use. Our initial tests had shown that it would be difficult to use the most powerful of them, like broadcast or WWV stations, because those radiate continuous wave signals with low-elevation radiation patterns. These features make it impossible to distinguish between the sky wave (ionosphere-reflected) and the ground wave modes of propagation at distances where the effect of multiple scattering should be observed. It is far preferable to use pulse signals of existing HF radars with vertically directed and horizontally polarized antennas. The original plan for this experiment was to use Platteville MF Radar as a signal source. This radar operates continuously radiating sixty 20 μsec pulses per second at the fixed frequency 2219 kHz [*Manson et al.*, 2003]. The inflexible selection of operating frequencies and a lack of possibility to synchronize phases between this radar and a remote receiver forced us to reconsider the original plan. The selection was made in favor of the recently installed Boulder VIPIR (Vertical Incidence Pulsed Ionosphere Radar) system (HF Radar built by Scion Associates Inc. [*Grubb et al.*, 2008]). The VIPIR provides several benefits: It allows one to use variable modes of operation, a possibility to work with a desirable set of frequencies and a possibility to implement phase synchronization between the radar's transmitter and the sensor's receiver. Eventually this transition proved to be very successful.

[19] Boulder VIPIR shares the transmitting antenna with a colocated Digisonde. This is a crossed delta antenna with a smaller delta currently inactive. The antenna provides a reg-

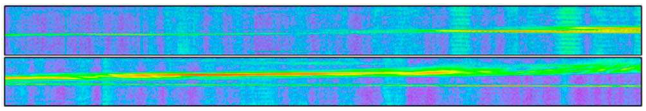

Figure 3. Amplitude of a received signal expressed in dB (blue corresponds to the minimum value; red corresponds to the maximum value) calculated from raw I and Q data provided in two consecutive VIPIR recordings, (top) BD840_2009310012019 and (bottom) BD840_2009310012523 (bottom panel), for channel #3, frequency #4. Both axes are time axes, with, however, rather different scales: vertical position of each pixel corresponds to the time of arrival of a signal within receiver's ~5 msec window open after each pulse; horizontal position corresponds to a consecutive number of the interpulse period within the sounding session, the total duration of which was 4.5 min. Ionospheric reflections are represented by easily identified bright strips stretched in the horizontal direction. Vertical features manifest radio interference.

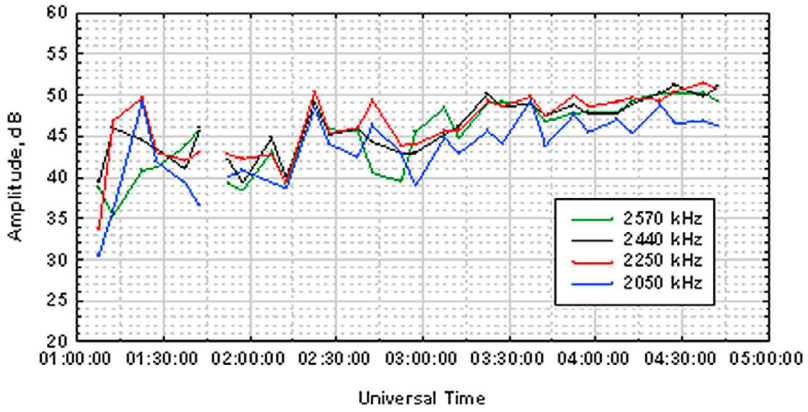

Figure 4. Smoothed (over the recording's length) amplitude of the signals reflected from the ionosphere at four frequencies measured by Boulder VIPIR during a night experiment on 13 November 2009. The trend noticeable between 01:00 and 03:30 UT is caused by decreasing collisional absorption in the decaying post-sunset E layer.

ular pattern at the near-vertical incidence angles with a gradually decreasing gain at the takeoff angles important for detection of the ionospherically reflected signal up to 100 km ground distance.

[20] During our experiments, VIPIR was operated in a special mode. Two 4.5 min sounding sessions were scheduled each 15 min to not overlap with the Digisonde operation that took the remaining 5 min. The Digisonde ionograms have provided basic information about the ionosphere needed for data processing. During each sounding session the radar has continuously radiated 100 pulses per second with the pulse duration 60 μsec. Frequencies were changed from pulse to pulse, cycling through 4 values: 2050, 2727, 3388, 4171 kHz for day time and 2050, 2250, 2440, 2570 kHz for nighttime. The experiments were conducted in September–November 2009 in conditions of a prolonged solar minimum. The two sets of frequencies covered most of the band being able to reflect vertically from the ionospheric layers. Specific frequencies were chosen with minimal radio frequency interference.

[21] The described mode is equivalent to simultaneous ionospheric radio sounding at four fixed frequencies with a pulse repetition interval 0.04 s at each frequency.

[22] The VIPIR's eight-channel receiving system has produced recordings of the signal received at the position of VIPIR itself in its standard format. Each recording contains data of a single sounding session. Recordings provide 512 I and Q data readings taken after every radiated pulse for all eight channels with 10 μsec intervals (see examples of the raw data in Figure 3). The recordings were used in the data processing to measure the temporal trend of the ionospherically reflected signal caused by diurnal variations of both collisional absorption and noncollisional anomalous attenuation (see Figure 4).

[23] For detection of the spatial effect of multiple scattering it is necessary to use an appropriate MF/HF-band digital receiver connected to a computer and to have an ability to perform measurements at various locations within 0–125 km distance from the transmitter in a matter of hours. A car-mounted mobile installation meets these requirements. For the receiving part of this installation we have used an instrument developed by the LOIS Consortium, Sweden

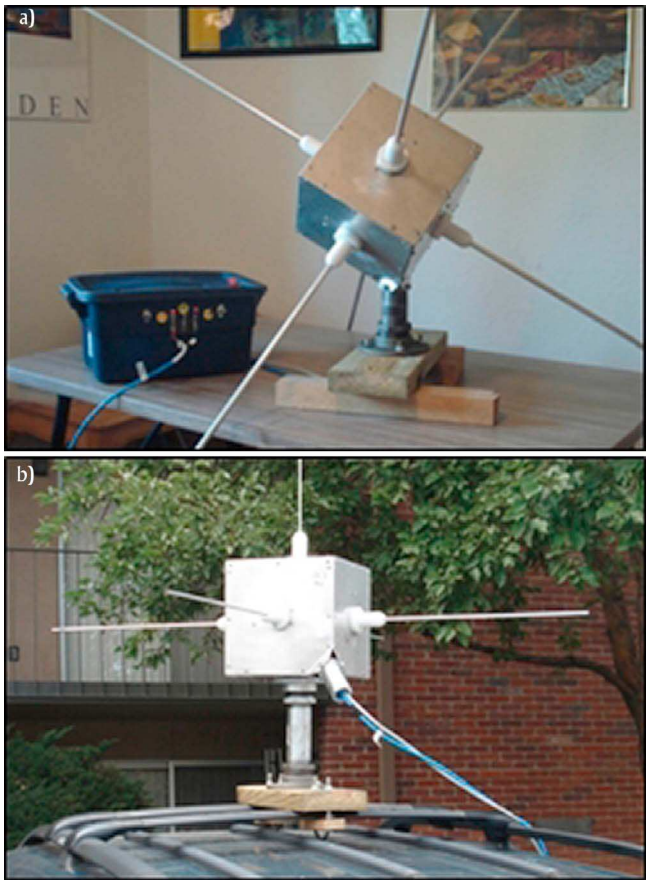

Figure 5. (a) Original configuration of the RVFS's tripole as used by Scandinavian LOIS project. Also shown is the battery unit intended for power supply of the RVFS in our experiments. (b) Modified antenna layout to provide a physical separation of the vertical and horizontal components of the radio field. The tripole is shown mounted on a car roof.

Figure 6. Map of the routes traveled by the mobile setup shown in the inset. Dimensions of the area shown are 130 (east-west) by 50 (south-north) km.

(Växjö University, the Swedish Institute of Space Physics, Uppsala division, and others) as part of their "outrigger" to the LOFAR system. This instrument is called the Radio Vector Field Sensor (RVFS). The RVFS consists of three-axis orthogonal electric dipoles (the "tripole"), all of small electrical size. They are active antennas, and are integrated with fully software-configurable three-channel digital receivers. The raw data output of the RVFS represents a sequence of I and Q data for the three antenna/receiver channels, obtained at a chosen central frequency and with a chosen bandwidth. The device has its own IP address and the data are accessible over an Ethernet connection.

[24] Original tripole layout had all dipoles rotationally symmetric with relation to the vertical axis (see Figure 5a). Each antenna output was a mix of the unweighted vertical and horizontal components of the radio field. While this was appropriate for a radio quiet location of the LOIS system in Scandinavia, this was unsuitable for the Boulder area where several powerful broadcast radio stations were in close vicinity. The unwanted vertical electrical component of the radio field in Boulder vicinity is usually much stronger than the horizontal electrical components of the wavefield of the expected ionospheric reflections. Frequently the vertical component of the ambient field caused saturation of all three channels. After some testing the tripole layout was changed to separate the vertical component of the field from the horizontal ones (see Figure 5b).

[25] Tests conducted in an RF-shielded room showed that commercial DC-DC power converters normally used in cars would be too noisy for our application. That is why a high-capacity battery unit has been used in our experiments to supply power to the RVFS (see Figure 5a). The laptop running control software has also been operated on its battery. To avoid a noise from the car's electrical system all measurements have been performed during short-time stops with the engine completely off. The stops have been coordinated in time with the VIPIR's sounding sessions.

[26] During a measurement session the sensor has been tuned by the software to each of the four frequencies radiated by VIPIR, in turn, for a fixed time interval, thus recording into a data file sequences of I and Q data corresponding to 75 radar pulses at each frequency. Time and location marks for each measurement session were provided to the control software by a commercial GPS receiver connected to the laptop through USB port.

[27] Routes traveled by the mobile setup during our field experiments were spanning ~20 km to the west and ~120 km to the east from Boulder (see map in Figure 6). The choice

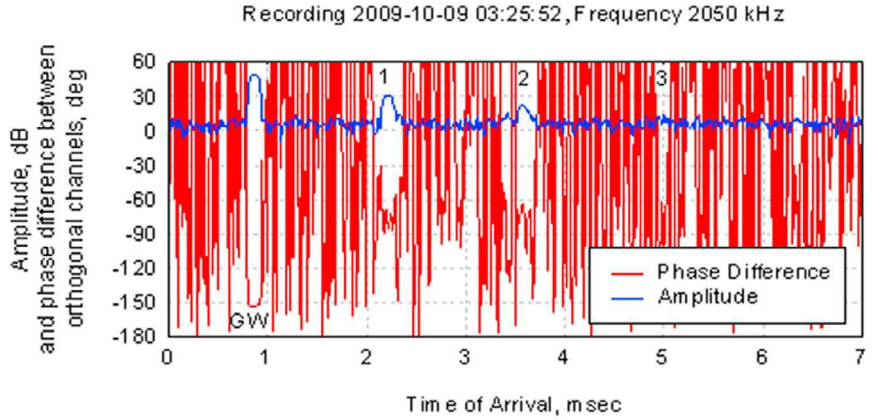

Figure 7. A result of the coherent summation of 75 interpulse periods for a single RVFS recording and a single frequency performed with a linear correction of the phase. Both amplitude of the horizontal field and the phase difference between two orthogonal horizontal channels are shown as functions of the gate number (time of arrival). Distinctive peaks correspond to the ground wave (GW) and to the multiple *F* region reflections of an ordinary wave (1, 2, 3).

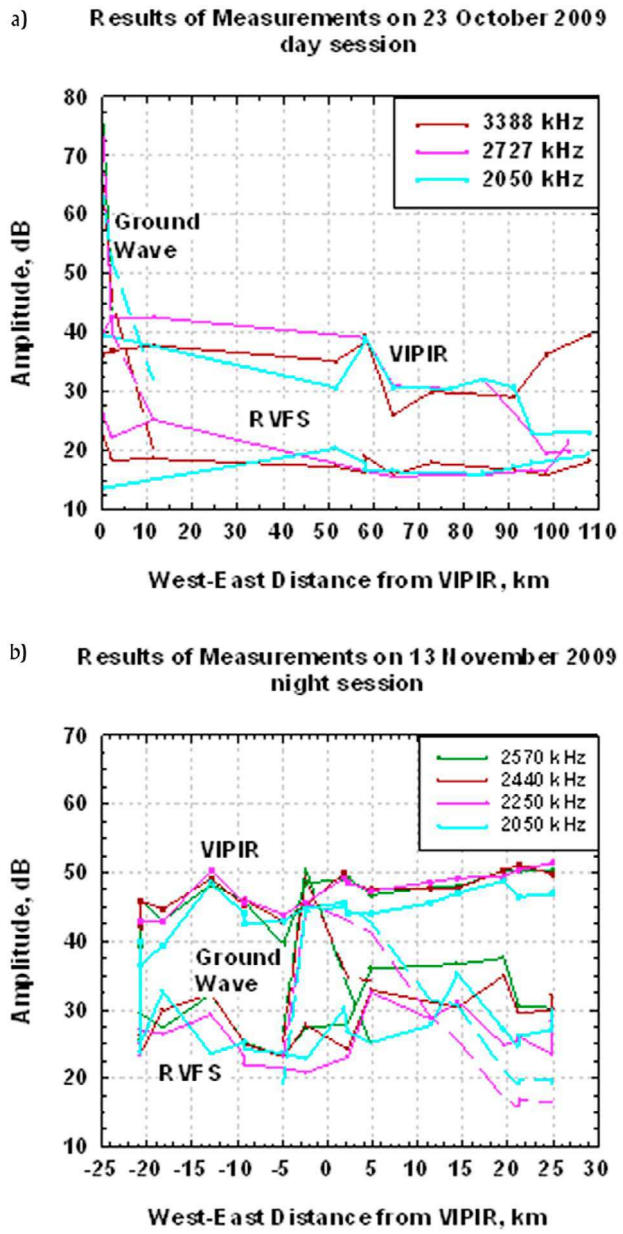

Figure 8. Results of the amplitude measurements for two series performed with RVFS: (a) on 23 October and (b) on 13 November 2009. Amplitudes of the ground waves are shown by dashed lines, and the amplitudes of the first ionospheric reflection at remote positions are shown by solid lines marked "RVFS." Also shown are results of simultaneous amplitude measurements made by VIPIR, which represent the variation in amplitude of the vertical incidence reflection with time, transposed to the spatial coordinate.

of the routes was justified by the predicted scale length of the studied effect which is smaller for the east-west direction. A few powerful broadcast radio stations, representing a saturation threat for the sensor, are located in Boulder and around Brighton. However, ~75% of the routes spans were sufficiently radio quiet. The measurements were performed during short-time stops at locations of opportunity along the routes, separated by irregular distances of the order of several kilometers. About 15 long-range rides have been made in October–November 2009.

4. Data Processing

[28] There are several factors that make measurements of the amplitudes of ionospheric reflections more challenging with the mobile RVFS compared to VIPIR. The RVFS dipoles are electrically small and these are placed too low over the ground and at a very small distance from the car's roof. The mobility requirements make the antenna layout suboptimal for detecting weak signals. Analog antenna preamplifiers, unavoidable in this situation, add a substantial internal noise into the receiving channels. To obtain an appropriate dynamic range in these conditions it was necessary to apply coherent techniques.

[29] The Tx and the Rx did not have means to maintain a phase lock. Internal reference frequency of the receivers has been calibrated in the beginning of every measurement series using strong ground wave signal from nearby VIPIR. However, it has not remained stable enough, supposedly because of environmental factors (solar heat, vibration). This and also the natural ionospheric Doppler effect have led to a variable rate of the phase shift between the radiated and the received pulses. To compensate for this trend the procedure of coherent summation of the pulses has been modified to include a phase correction of the linear kind

$$\delta p = \Delta\omega \cdot t,$$

where δp is the expected phase drift due to the reference frequency mismatch between the radar and the sensor, t is the time elapsed since the start of the measurement session, and $\Delta\omega$ is the value of the reference frequency mismatch between the radar and the sensor. No a priori assumptions have been made about $\Delta\omega$. An algorithm was applied automatically and individually for each recording and each frequency that selected a value of $\Delta\omega$ maximizing amplitudes of the ionospheric reflections yielded by the procedure of coherent summation of the signals. A typical result of this preprocessing is illustrated in Figure 7. This recording was made at a relatively short distance (5 km) from VIPIR. Both the ground wave (peak marked GW) and the multiple ionospheric reflections (numbered in the image) are easily determined here. A useful way to confirm correctness of this determination is checking the phase difference between two orthogonal horizontal channels (that should be around −90° for ordinary ionospheric echoes, around +90° for extraordinary echoes, and arbitrary for the ground wave). In case of uncertainty, the Digisonde ionograms provide additional clarifying information about near-vertical propagation times of the signals.

[30] Figures 8a and 8b show results of the amplitude measurements for two series performed with RVFS on 23 October and 13 November 2009. Only results related to the ground wave and the first ionospheric reflection are shown. One can see that it was easy to distinguish the two also by their corresponding dependence on the distance from VIPIR: The ground wave signal was decreasing steeply and dropped below the RVFS noise floor for the distances larger

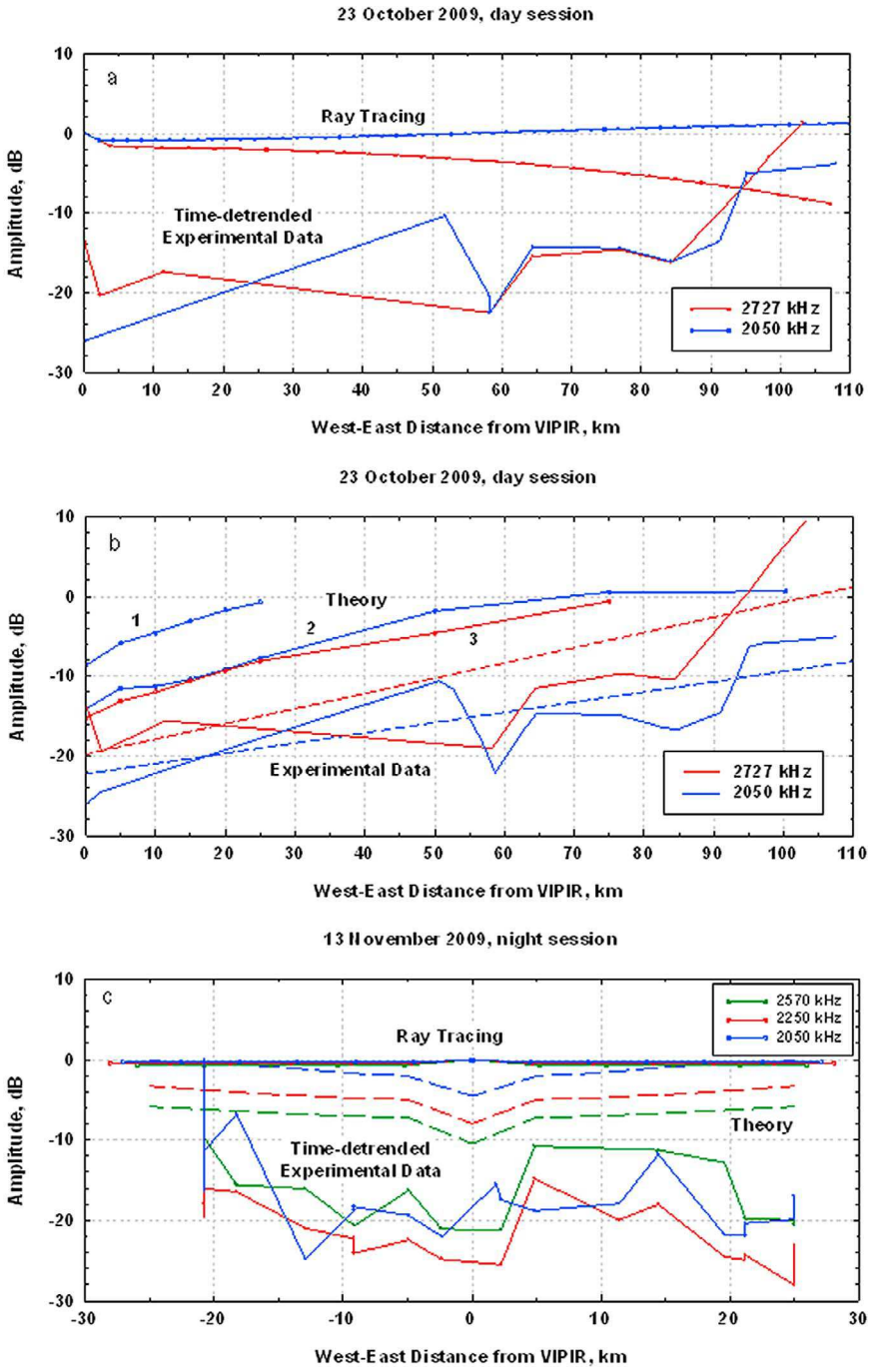

Figure 9. The time-detrended values of the signal amplitude measured with RVFS are compared with the results of ray tracing calculations for the series (a) of 23 October 2009 and (c) of 13 November 2009. (b) The difference between the experimental amplitude distribution and the ray tracing results for the series of 23 October 2009 is compared with the shape of function (equation (2)) predicted by the theory of multiple scattering. The experimental curves are accompanied by their linear fits (shown by dashed lines). The three theoretical plots correspond to the different sets of parameters: 1, $f = 2050$ kHz, $\nu = 2.7$, $\Delta N/N = 0.01$, $H = 20$ km; 2, $f = 2050$ kHz, $\nu = 2.7$, $\Delta N/N = 0.02$, $H = 20$ km; 3, $f = 2727$ kHz, $\nu = 2.7$, $\Delta N/N = 0.005$, $H = 50$ km. For the series of 13 November 2009 this comparison is done in Figure 9c, and the three theoretical plots shown by dashed lines correspond to the following sets of parameters (from the top down): $f = 2570$ kHz, $\nu = 2.2$, $\Delta N/N = 0.005$, $H = 50$ km; $f = 2570$ kHz, $\nu = 2.7$, $\Delta N/N = 0.005$, $H = 50$ km; $f = 2570$ kHz, $\nu = 3.0$, $\Delta N/N = 0.005$, $H = 50$ km.

than 20–25 km. This distance for the westbound leg of the routes crossing mountains was much shorter, about 5–7 km. The amplitude data provided by the VIPIR for the purposes of this illustration and for further analysis has been converted from time domain into spatial domain: these are shown as functions of the distance to VIPIR the mobile setup had at the time of measurement. Ideally, the VIPIR amplitudes should be plotted on a time axis, but this might not look very good because distance is not linear with time. Amplitudes measured by VIPIR have higher values compared to the ones provided by RVFS because VIPIR has greater sensitivity and lower noise. For purposes of this work we express all amplitudes in dBs and pay attention only to the shapes of the curves, but not to their absolute positions.

[31] There are only few steps left to come to physical conclusions. First of all, we would like to get rid of a purely temporal trend if it is present in the RVFS results, since we are interested in spatial effects. Such propagation conditions as collisional absorption in the ionosphere may change during the 4–5 h time interval when a measurement series is done. Objective information about this trend has been provided by the VIPIR data since its measurements were performed in a fixed location. To compensate for the temporal trend, we subtract the VIPIR amplitudes from the RVFS amplitudes when both are expressed in dB. The results are shown in Figures 9a and 9c and these demonstrate a clear tendency to have a minimum near the VIPIR position and to increase with the distance.

5. Discussion

[32] The property of a signal to have a minimum near the VIPIR position and to increase with the distance is not an effect of ray theory. Figures 9a and 9c show results of ray tracing calculations that have been done using electron density profiles obtained by Digisonde ionogram inversion program ARTIST4 for the time periods of measurement series and a conventional model for electron collision frequency profile. These calculations take into account both spatial divergence of the rays and the collisional absorption in the layered ionospheric plasma. For the conditions of our experiment the ratio of the electron collision frequency to the radio frequency at the vertical reflection level did not exceed 0.025, so the effect of collisional attenuation on the raypath itself could be neglected. Dependence of the VIPIR's transmitting antenna gain on the off-vertical angles was calculated by 4nec2 program and was also taken into account as a factor influencing the signal amplitudes. What is shown in the Figures 9a and 9c is the difference (in dB) of the expected amplitudes of ionospheric reflections at some distance from VIPIR and at the VIPIR's location. One can see that geometrical optics predicts either almost constant or slightly decreasing amplitudes of the signals in the 0–100 km range of distances from the source.

[33] After subtraction of the ray tracing values from the time-detrended experimental results, one obtains amplitude dependencies (expressed in dB versus distance) which shapes may be compared directly with the results of theoretical calculations of function L described in section 2. For the measurement conducted on 23 October 2009 this comparison is done in Figure 9b. In addition to the two experimental plots obtained using the above correction procedure and found in the bottom of Figure 9b, three theoretical curves are shown corresponding to two different frequencies and to different values of the layer thickness and the irregularity amplitude. What should be compared are the general slopes of the theoretical and experimental plots. Vertical positions of the plots differ because amplitude measurements performed by the two different instruments were not intercalibrated. For the experimental plots we facilitate the comparison by providing the linear fits (shown by dashed lines). One can see that parameters of the theoretical calculations can be adjusted to approach an approximate correspondence of the slopes of theoretical and experimental plots. The difference in the variation with distance between the two frequencies (2050 and 2727 kHz) is explained by much closer proximity of the second frequency to the critical frequency of the E layer determined from ionograms. For the conditions of 13 November 2009 the ray tracing values are almost flat versus the distance, so we do not perform the subtraction and the comparison with the theoretical estimates is done directly in Figure 9c. The three theoretical plots correspond in this case to a single frequency 2570 kHz and to different values of the irregularity spectrum index. The general tendency revealed by the theory, for the amplitude to have a minimum at the source location, is reproduced qualitatively by the experimental curves, though characteristic scale lengths may differ quantitatively. These differences may be due to simplifications in the theory (a linear background layer of the ionospheric plasma was assumed, and influence of the magnetic field on the radio wave's refractive index was neglected in the calculations).

[34] Parameters of the spectrum of irregularities (the spectral amplitude and the spectral index) may vary significantly from day to day (and even more rapidly) in the scale length band of interest (0.1–5 km). Therefore it should not be expected that the spatial effects of the multiple scattering can be observed easily every time the measurements are performed. This work demonstrates that the observed amplitudes of ionosphere reflections frequently deviate substantially from the predictions of geometric optics. Note that scattering represents the only factor limiting applicability of the geometrical optics approximation. And it is important that deviations observed in our experiments are of the type that can be described by the theory of multiple scattering.

[35] A brief consideration should be given to the random variations of the signal amplitude noticeable in the experimental plots of Figures 8 and 9. The most likely reason for them is interaction of the sounding signal with large-scale (few tens kilometers) irregularities producing the interference pattern on the ground which correlation scale is comparable to the transmitter-receiver separation. Temporal variations of the spectral amplitude and the spectral index of the ionospheric irregularities could be responsible for this effect in Figure 8, but not in Figure 9: amplitudes provided by the two devices should be affected by this mechanism equally.

6. Conclusion

[36] This paper presents results of an experimental campaign that was conducted in September–November 2009 in

and around Boulder, CO. The purpose of this campaign was to confirm specific predictions of the theory of multiple scattering of a spatial distribution in the amplitude of ionospherically reflected signal in presence of intermediate-scale (0.1–5 km) irregularities in the ionosphere. The signal was radiated by the new Boulder VIPIR system and the amplitude of ionospheric reflection was measured both by VIPIR and by a mobile setup including Radio Vector Field Sensor, a digital receiving system capable to measure all three components of the radio field.

[37] The experiment required alleviation of several unfavorable factors. These included unavoidably suboptimal characteristics of the mobile receiving system, presence in the area of several unwanted strong transmissions, and inherent variability of the ionosphere. Because of varying level of the ionospheric irregularities, the wanted effect was not expected to manifest itself in every measurement session. We desired a better statistics to obtain a more definitive support for the theory. Nevertheless, the results obtained do confirm the occurrence of significant deviations in the distribution of the average amplitude of ionosphere reflections on the ground from the predictions of geometrical optics. Fundamentally important, geometric optics cannot explain these results, and the deviations observed can be explained by the theory of multiple scattering in the ionosphere. Combined with experimental evidence obtained earlier, our new results provide a significant contribution into validation of the multiple scattering theory.

[38] The experimental campaign was conducted in conditions of the prolonged solar minimum causing low densities of the ionospheric plasma which limited substantially the radio frequency band that could be used in the experiments. The theory of multiple scattering generally predicts stronger effects for higher radio frequencies. In addition, higher levels of ionospheric irregularities are associated with increased solar activity. This justifies planning a follow on experimental campaign using similar techniques. In the next campaign the amplitude measurements should be complemented with direct measurements of the irregularity spectrum that can be provided by VIPIR using Phase Structure Function method.

[39] **Acknowledgments.** This project has been supported by NSF through ATM-0737625 award. The authors appreciate the assistance of L. Zabotina in conducting experiments, of G. Zhbankov in performing ray tracing calculations, and of J. W. Wright in assembling initial version of the mobile setup. Numerical calculations for this project were performed using high-performance computational facilities of the National Center for Atmospheric Research. An RF-shielded room facility of the CU Boulder/NOAA's Center for Environmental Technologies has been used.

References

Baulch, R. N. E., E. C. Butcher, J. C. Devlin, and P. R. Hammer (1984), A simple sounder to measure the properties of ionospherically reflected radio waves, *J. Atmos. Terr. Phys.*, *46*, 895–903, doi:10.1016/0021-9169(84)90029-1.

Belikovich, V. V., E. A. Benediktov, N. P. Goncharov, and A. V. Tolmacheva (1997), Diagnostics of the ionosphere and neutral atmosphere at *E* region heights using artificial periodic inhomogeneities, *J. Atmos. Sol. Terr. Phys.*, *59*(18), 2447–2460, doi:10.1016/S1364-6826(96)00139-3.

Boiko, G. N., et al. (1984), Artificial defocusing lens in the ionosphere, *Sov. Phys. JETP*, Engl. Transl., *39*, 652–655.

Boiko, G. N., et al. (1985), Analysis of the defocusing of radio waves in the ionosphere due to the influence of an intense radio-frequency radiation field, *Radiophys. Quantum Electron.*, Engl. Transl., *28*, 655–665.

Bronin, A. G., and N. A. Zabotin (1992), The equation of radiation energy transfer in an irregular magnetized plasma, *Sov. Phys. JETP*, Engl. Transl., *75*(4), 633–638.

Bronin, A. G., and N. A. Zabotin (1993), Reduction of radiation transfer equation to invariant variables for randomly inhomogeneous plain-stratified magnetoactive plasma, *Radiophys. Quantum Electron.*, Engl. Transl., *36*, 869–871.

Bronin, A. G., P. F. Denisenko, and N. A. Zabotin (1993), Attenuation of the decameter wave field coherent component at vertical sounding of the ionosphere as a result of scattering on random irregularities, *Geomagn. Aeron.*, Engl. Transl., *33*(1), 141–143.

Bronin, A. G., N. A. Zabotin, and Y. N. Cherkashin (1996), An analytic approach to estimating the optical thickness of the ionospheric plasma layer in vertical sounding, *Geomagn. Aeron.*, Engl. Transl., *36*(4), 495–499.

Bronin, A. G., N. A. Zabotin, G. A. Zhbankov, and E. V. Kuznetsov (1998), Influence of small-scale ionospheric irregular structure on the spatial-and-angular distribution of radiation in the vicinity of sounding station, *Geomagn. Aeron.*, Engl. Transl., *38*(3), 347–353.

Bronin, A. G., N. A. Zabotin, and E. S. Kovalenko (1999), Nonmonochromatic radiation transfer in a plane slab of magnetized plasma with random irregularities, *Radio Sci.*, *34*(5), 1321–1328, doi:10.1029/1999RS900064.

Denisenko, P. F., V. I. Vodolazkin, Y. N. Faer, and L. N. Boltykhova (1987), Anomalous absorption of radio waves and the effective electron collision frequency in the ionosphere F region, *Geomagn. Aeron., Engl. Transl.*, *27*(3), 438–440.

Godin, O. A. (2009), Stability of acoustic wave fronts propagating in anisotropic three-dimensional environments, *Acta Acust. Acust.*, *95*, 963–974, doi:10.3813/AAA.918228.

Grubb, R. N., R. Livingston, and T. W. Bullett (2008), A new general purpose high performance HF radar, paper presented at XXIX URSI General Assembly, Union Radio Sci. Int., Chicago, Ill.

Jones, T. B., T. R. Robinson, P. Stubbe, and H. Kopka (1984), Frequency dependence of anomalous absorption caused by high power radio waves, *J. Atmos. Terr. Phys.*, *46*, 147–153 http://dx.doi.org/10.1016/0021-9169(84)90140-5, doi:10.1016/0021-9169(84)90140-5.

Kovalenko, E. S., and N. A. Zabotin (1999), Multiple scattering effects in vertical sounding of equatorial ionosphere, *J. Atmos. Sol. Terr. Phys.*, *61*, 1059–1066, doi:10.1016/S1364-6826(99)00050-4.

Manson, A. H., C. E. Meek, S. K. Avery, and D. Thorsen (2003), Ionospheric and dynamical characteristics of the mesosphere-lower thermosphere region over Platteville (40°N, 105°W) and comparisons with the region over Saskatoon (52°N, 107°W), *J. Geophys. Res.*, *108*(D13), 4398, doi:10.1029/2002JD002835.

Setty, C. S. G. K. (1972), Electron collision frequency in the ionospheric layers, *Indian J. Radio Space Phys.*, *1*, 38–51.

Setty, C. S. G. K., A. R. Jain, and M. K. Vyawahare (1970), Collision frequency of electrons in F-region, *Can. J. Phys.*, *48*, 653–658, doi:10.1139/p70-084.

Setty, C. S. G. K., O. P. Nagpal, and V. K. Dhawan (1971), Variation of electronic collision frequency in the F-region, *Indian J. Pure Appl. Phys.*, *9*, 519–521.

Vas'kov, V. V., and A. V. Gurevich (1975), Nonlinear resonant instability of a plasma in the field of an ordinary electromagnetic wave, *Sov. Phys. JETP*, Engl. Transl., *42*(1), 91–97.

Vodolazkin, V. I., P. F. Denisenko, V. P. Rzhanitsyn, V. V. Sotskij, and Y. N. Faer (1993), Absorption of radio waves and the effective electron collision frequency in the midlatitude ionosphere, *Geomagn. Aeron.*, Engl. Transl., *33*(3), 336–342.

Yerukhimov, L. M., G. P. Komrakov, and V. L. Frolov (1980), Spectrum of small-scale artificial ionospheric turbulence, *Geomagn. Aeron.*, Engl. Transl., *20*, 783–784.

Zabotin, N. A. (1993), Radiofrequency radiation energy transfer in an ionospheric layer with random small-scale inhomogeneities, *Radiophys. Quantum Electron.*, Engl. Transl., *36*, 813–820.

Zabotin, N. A., and E. S. Kovalenko (1999), Simple numerical model of radio wave multiple scattering effects in the ionospheric plasma layer, *Waves Random Media*, *9*, 393–399, doi:10.1088/0959-7174/9/3/307.

Zabotin, N. A., and J. W. Wright (2001), Ionospheric irregularity diagnostics from the phase structure functions of MF/HF radio echoes, *Radio Sci.*, *36*(4), 757–771, doi:10.1029/2000RS002512.

Zabotin, N. A., A. G. Bronin, and G. A. Zhbankov (1998a), The radiation transfer at a layer of magnetized plasma with random irregularities, *Waves Random Media*, *8*, 421–436, doi:10.1088/0959-7174/8/4/003.

Zabotin, N. A., A. G. Bronin, and G. A. Zhbankov (1998b), Reflection of a radio sounding signal from a plasma layer with random irregularities, *J. Commun. Technol. Electron.*, Engl. Transl., *43*(7), 799–807.

Zabotin, N. A., A. G. Bronin, and E. S. Kovalenko (2001), Group propagation time of quasi-monochromatic radiation in a plane layer of plasma with random irregularities, *Radio Sci.*, *36*(5), 1093–1102, doi:10.1029/2000RS002559.

Zabotin, N. A., A. G. Bronin, G. A. Zhbankov, V. L. Frolov, G. P. Komrakov, N. A. Mityakov, and E. N. Sergeev (2002), Anomalous attenuation of extraordinary waves in ionosphere heating experiments, *Radio Sci.*, *37*(6), 1102, doi:10.1029/2000RS002609.

Zabotin, N. A., J. W. Wright, and E. S. Kovalenko (2004), Multiple scattering effects in ionospheric radio sounding, *Radio Sci.*, *39*, RS3002, doi:10.1029/2003RS002953.

T. Bullett and N. Zabotin, CIRES, University of Colorado at Boulder, 425 UCB Boulder, CO 80309-0425, USA. (nikolay.zabotin@gmail.com)